SEISMIC RESISTANCE OF REINFORCED CONCRETE-MASONRY SHEAR WALLS WITH HIGH STEEL PERCENTAGES

M. J. N. Priestley*

ABSTRACT

This paper summarizes test results of six heavily reinforced concrete masonry shear walls. The test programme was designed to investigate the necessity for the low ultimate shear stress specified by Masonry codes. Care was taken to accurately model good, but realistic design practice in detailing, and variables investigated in the series included steel percentage, influence of vertical load and confinement of potential crushing areas by mortar bed confining plates.

Results are presented which clearly indicate that the maximum current code allowance for ultimate shear stress is unreasonably low. No wall suffered diagonal shear failure despite maximum shear stresses exceeding four times the maximum code level. All walls displayed stable hysteresis loops at a displacement ductility factor of 2, and the less heavily reinforced walls (designed to approximately twice code levels) were satisfactory at DF = 4. Degradation was never catastrophic and occurred due to slip of the entire wall along the foundation beam. Methods for reducing the degradation are discussed. Confining plates did not significantly reduce the degradation of the hysteresis loops, but substantially reduced damage to the walls at high ductility factors.

Values of required ductility for walls designed to the Loadings Code are investigated, and on the basis of these and the experimental results, recommendations are made for relaxation to the ultimate shear provisions of the masonry code.

1. INTRODUCTION

1.1 Allowable Shear Stresses

The research described in this report was carried out for one main purpose: to establish that the maximum shear stresses allowed for masonry structures by existing[1] and proposed draft[2] N.Z. Masonry codes are unrealistically low. This is of considerable importance, as recent changes in design philosophy which have been incorporated in the recently adopted Loadings code (NZS 4203)[3], together with the concepts of capacity design have resulted in the situation where many structures of four or more storeys cannot be designed in reinforced masonry because of the shear limitations.

Consider the situation of a building designed for Zone A[3] using external masonry shear wall elements. Assume the aspect ratio (height/width) of the walls is less than 2.0.

NZS 4203 Requirements

The required base shear capacity is

$$V = C_d \cdot W_t$$

where C_d = C S M I R

and W_t = seismic weight

C = 0.15 (period will generally be less than 0.5 sec)

S = 1.6 (squat shear wall)

M = 1.2 (masonry)

I = 1.0 (assuming no special importance)

R = 1.0

$\therefore$ $C_d = 0.288$

and $V = 0.288\ W_t$.

Thus the flexural strength would be based on a seismic coefficient of 0.288. An undercapacity factor of 0.65 is required[2] for design for flexure in combination with axial load. If grade 380 steel is used for vertical reinforcement, an overcapacity factor of 1.35 would be appropriate for shear design.

Thus the ratio

$$\frac{\text{required shear strength}}{\text{required flexural strength}} = \frac{1}{0.65} \times 1.35 = 2.08$$

Consequently, the equivalent seismic coefficient for shear for the above example would be $Cd_s = 0.288 \times 2.08 = 0.60$.

It is apparent that comparatively high shear stresses will be required to meet this demand. Looking at the requirements from a different viewpoint, these figures imply that the maximum allowable shear stress associated with the design seismic coefficient ($C_d = 0.288$) must be

$$v_u \leq \frac{1}{2.08} \times \text{Code max shear stress},$$

to avoid the possibility of a shear failure. It could be argued that an S = 1.6 structure

* Senior Lecturer in Civil Engineering, University of Canterbury.

does not need an overcapacity approach for shear, as flexural yielding is not required by NZS 4203 for this class of structure. However, the writer believes that this would be unsafe, as the rapid reduction in strength, and the absence of 'significant' energy absorption, associated with shear yielding could have catastrophic consequences.

The proposed draft Masonry Code[2] allows a maximum shear stress of $.15\sqrt{f'm}$, with a maximum of .62 MPa. This amounts to 0.43 MPa if masonry prisms are not tested (f'm = 8.3 MPa assumed), and a maximum shear stress of 0.62 MPa for masonry prisms giving crushing strengths f'm > 17.2 MPa. Thus the maximum allowed shear stresses associated with the design seismic coefficient (.288 in the example above) are

for f'm = 8.3 MPa , $v_u \leq 0.21$ MPa

for f'm $\geq$ 17.2 MPa , $v_u \leq 0.30$ MPa

These restrictions are clearly very limiting.

1.2 Actual Shear Strength

Past research by Scrivener[4] and Schneider[5] on Concrete Masonry walls indicated that shear strength was independent of shear steel content. Dependable values exceeding 1.0 MPa were obtained, but much of previous testing was of monotonic nature rather than cyclic load reversals. In a recent paper on Brick Masonry Shear Walls[6] the writer noted that neither Scrivener nor Schneider had included sufficient shear steel to carry the full shear load associated with flexural failure. Paulay[7] in discussing shear strength of reinforced concrete walls noted the necessity to provide shear steel to carry the total shear load in hinging regions under seismic load.

The results from Brick Masonry wall panels[6] indicated that high ultimate shear stresses could be obtained, and flexural failures induced, if adequate shear steel was provided. It was expected that the results would be equally applicable to Concrete Masonry, but it was felt advisable to confirm by testing.

1.3 Realistic Construction Methods

Much of the previously published data was based on wall units constructed in rather different fashion to that used in practice. Because of this, it was felt necessary to test wall units of realistic construction, including

(1) Reinforced concrete foundation beams with starter bars for vertical reinforcing;
(2) Lapping of vertical steel within the reinforcing, at the wall base;
(3) Use of open-end bond-beam units in the wall;
(4) Inclusion of clean-out ports in the bottom course of blocks.

Items 2 and 4 were expected to accentuate any tendency for face shells to separate from the webs and grout core during high level loading.

1.4 Mortar Bed Confining Plates

Tests on Brick Masonry walls under cyclic loading[6] indicated that significant improvement in inelastic behaviour was obtained if toe and heel areas were confined by the inclusion of thin stainless steel plates in the mortar beds over the bottom few courses. It was expected that similar enhancement of behaviour would result for concrete masonry walls, but experimental verification was required.

The experimental work described in this paper reflected these apparent research needs, and was directed towards an initial investigation of the shear strength and general structural performance of heavily reinforced concrete masonry walls constructed in realistic fashion, with and without mortar bed confining plates. Complete test details are available in Ref. 8.

2. DESCRIPTION OF TEST UNITS

Basis of Test Design.

The prototype conditions to be modelled represented a class S = 1.6[3] shear wall, that is, a wall with aspect ratio (height/base width) less than 2. It was felt that the minimum aspect ratio of interest was 1.0, and as this would represent more critical conditions for shear than higher walls, the wall units should represent a prototype aspect ratio close to unity.

In the tests it was necessary to apply the horizontal shear load as a single point load at the top of the wall, whereas in reality seismic loads will result from the mass of each floor and the roof. As shown in the simplified representation of a four-storey structure in Fig. 1, modelling the correct ratio of Shear to Bending Moment in the critical first storey requires that the equivalent single load be applied at a height of about 2.75 x storey height, or 69% of the total building height. Consequently to model a prototype wall of unit aspect ratio, the model panel should have less than unit aspect ratio.

Fig. 2 shows the wall dimensions adopted, resulting in an aspect ratio of 0.75, which in terms of the example in Fig. 1 would represent a prototype aspect ratio of 1.09. The dimensions of the walls are such that block size is sufficiently small compared with panel size, and the wall height is adequate to avoid flexural steel bond failure. The design included a large reinforced concrete bond beam of high axial stiffness relative to the shear stiffness of the wall, to minimize arching action during initial stages of load application.

143mm wide concrete blocks were adopted for the tests to ensure that high shear stresses could be applied within the maximum load restrictions. With the test design maximum load set at 1 MN by the reaction frame design, maximum shear stresses of 2.87 MPa, or 4.8 times the maximum code shear could be applied.

Reinforcement Details.

Walls A1, A3, A5 and A6 contained 8 vertical 19.05mm diameter (No. 6) Grade 380 deformed bars as vertical (flexural) reinforc-

ing and the same amount of similar steel as horizontal (shear) reinforcing.

Walls A2 and A4 were less heavily reinforced, containing 6, 15.9mm diameter (No. 5) grade 380 deformed bars as flexural reinforcing, and 8, 15.9mm diameter (No. 5) grade 380 bars as shear reinforcing.

Walls A3, A4 and A6 differed from A1, A2 and A5 respectively only by the inclusion of 2.5mm thick stainless steel plates in the bottom three mortar courses. Dimensions of these confining plates are given in Fig. 3.

Walls A1 to A4 were tested without externally applied vertical load, as this was expected to be the critical condition for ultimate shear strength. However, Walls A5 and A6 duplicated Walls A1 and A3 respectively, but with an externally applied vertical load of 240 kN, providing an average compression of 0.69 MPa in the walls.

Vertical steel starter bars were welded to a steel angle-section cast in the bottom of the foundation beam, and all bars were lapped for a length of 54 bar diameters, starting at the level of the wall base. This represents current design practice, and produces maximum congestion at the wall base, thus reducing the effectiveness of the grout core in the critical region. All shear steel was hooked around the end vertical flexural bars. Tight bends (0.75 D radius) were necessary because of the limited grout space in the 143mm wide blocks. Table 1 summarizes reinforcing details.

Wall Construction.

Open-end bond-beam blocks (Winstones SI type 614) were used throughout the wall height as is current Ministry of Works and Development practice, as this allowed transverse steel at all levels, and provided the greatest continunity of the grout core. It also creates the weakest connection between opposite face shells, and would thus presumably be more susceptible to damage due to differential block movements. Two clean-out ports were provided in the bottom layer of blocks, and 614 blocks in this course were laid inverted to facilitate clean-out operations. All cells were filled by pumping ready-mix grout into the walls. Grout was vibrated once by insertion vibrator after a wall was half filled, and then left to settle while the other walls were half filled and vibrated. The walls were then completely filled and revibrated.

The blocklayer was asked to comment on any difficulties associated with incorporating the confining plates in the lower mortar bed. He found no special difficulties, though use of a finer mortar sand would have eliminated minor problems resulting from the reduced mortar bend thickness and large sand particles. The plates were found to be helpful in the second course in providing a bridge over missing clean-out face shells.

Material Properties.

Average material properties from samples of reinforcement, blocks, mortar and grout for all walls are listed in Table 2. Also given are results from three-course masonry prisms constructed with the walls.

It will be noted that the steel strengths, particularly for the 19mm bar are substantially higher than the minimum specified value. In the most extreme case, wall A1, the yield strength of the flexural steel is 27.5% above the nominal 414 MPa level (60 KSI) or 39% above the current design level for high strength steel of 380 MPa.

Mortar strengths were unexpectedly high, as a result of the adoption of a higher than specified cement/sand ratio by the blocklayer. However, tests[8] on grouted prisms with varying cement/sand ratios indicated that the influence on prism strength and failure behaviour was not particularly significant.

3. TESTING DETAILS

Load Application.

Racking load was applied to the walls by jacking between a specially constructed reaction frame and the near end of the wall ('compression' loading) or by jacking between strong-backs at the far end of the wall and the back of the reaction frame through two 32mm dia. Macalloy tension rods ('tension' loading). Vertical loads were applied to walls A5 and A6 through three 20-tonne jacks reacting against a vertical reaction frame anchored to strong-floor tie-down points. The three jacks were manifolded to a single pressure system, thus ensuring equal vertical load from each jack. Fig. 4 shows wall A5 under 'tension' load and vertical load.

Measurements

A IMN load cell monitored racking loads to a precision of 0.4 kN. Vertical load was monitored through a pressure gauge on the independent jacking system used for vertical loads. The estimated accuracy of +5% was adequate, as results were not particularly sensitive to the vertical load.

Displacements were monitored at the level of load application on both sides of the wall; at the base of the wall (to investigate slip of the wall on the foundation beam) and on the foundation beam itself (to monitor slip of the entire wall unit on the strong-floor. Readings from this dialgauge were subtracted from displacements at the level of load application, to obtain true wall deflection readings. Mitutoyo 50mm x 0.1mm dialgauges were used throughout.

Prior to testing, one side of each wall was painted with white undercoat to facilitate crack detection. Cracks were marked at each increment of loading, and photographed at displacement peaks.

Testing.

All walls were subjected to the same testing regime. Initially, the test unit was 'tension' loaded to a maximum load of approximately 70% of the theoretical ultimate moment capacity, based on measured material properties. The load was then removed and the wall 'compression' loaded to the same load level. The yield displacement was defined as the intersection of the initial load-deflection curve in the

post-cracking stage, with the theoretical ultimate load capacity, as illustrated in Fig. 5.

Following the initial 'elastic' cycle the wall was subjected to two full cycles to a displacement ductility factor of 2 (DF = 2; maximum displacement = 2 x yield displacement) then two full cycles to DF = 4, and so on. If the wall exhibited marked load degradation at any level of ductility it was subjected to a third cycle to that displacement. Walls A1 to A4 were then subjected to a final displacement controlled 'tension' load to failure, which was assumed to have occurred when load started decreasing with increased displacement.

4. RESULTS

Load-Deflection.

The behaviour of each wall under cyclic loading is illustrated by the load-deflection hysteresis loops of Fig. 6. For each wall theoretical ultimate load (P_u) and theoretical load at which the extreme tension bar first yields (P_y), based on measured material properties, are indicated. Displacement ductility factors, based on the 'yield' displacement defined above, are marked as DF = 2, DF = 4 etc. The following characteristics are apparent:

(1) In all cases the initial 'elastic' cycle to approximately 70% P_u is comparatively wide, indicating high elastic damping.

(2) All walls exceeded their theoretical ultimate capacity due to strain hardening of the vertical reinforcement.

(3) Load degradation on successive cycles at DF = 2 was small for all walls, and for walls A2 and A4, with lower reinforcement ratios, behaviour was satisfactory at DF = 4.

(4) On increasing the amplitude of cyclic displacement from DF = 2 to DF = 4, all walls attained an initial maximum load in excess of the value first reached at DF = 2, indicating that stiffness degradation rather than load degradation was responsible for reduction in successive peak loads at DF = 2.

(5) The heavily reinforced walls (A1, A3, A5, A6) suffered rapid degradation at DF = 4, but the walls with vertical load (A5 and A6) showed better performance than those without vertical load, despite the higher maximum loads attained.

(6) Behaviour at moderate ductility levels is similar to Clough's 'degrading-stiffness' model[9].

(7) Walls with confining plates (A3, A4, A6) did not exhibit significantly better performance than their unconfined counterparts (A1, A2, A5).

Base-Slippage.

It was observed that the cause of stiffness degradation at DF = 4 and higher displacement ductilities was largely caused by sliding displacement of the entire wall along the foundation beam (base-course slip) at low load levels. Similar behaviour was noted in earlier tests on brick masonry walls[6].

The mechanism appears to be as follows:

After the wall has suffered significant inelastic displacement in one direction, inelastic steel strains result in a wide open crack at the base course on removal of the load. As the load direction is reversed, the crack becomes open over the full length of the wall. Since the base mortar course is very smooth, aggregate interlock is totally ineffective, and all shear has to be resisted by dowel action of the vertical steel. This is known to be rather ineffectual, as significant sliding displacements are necessary to develop adequate shear resistance. As the load is increased, the compression steel yields, the base crack closes at the compression end, and shear can once more be transmitted across the compression zone of the blockwork. Consequently sliding creases, and the load level rises rapidly. This behaviour is apparent in all walls tested in this series.

It is of interest to examine the extent of base-course slip and compare with total displacements. Fig. 7 shows load vs base course slip graphs for walls A3, A4 and A6. In these graphs the ductility factor associated with each peak is marked (e.g. DF4), together with the number of the cycle at that displacement level, in parenthesis. The following points are noted.

(1) The curves all show characteristics of a stiffening spring - most of the base slip occurs at low loads. As the load increases and the base crack closes at the compression end, slip virtually ceases, as mentioned above. The base-slip remains effectively constant as the load is decreased.

(2) At DF = 2, base-course slip is a comparatively small proportion of the total displacement. (Compare with load-displacement hysteresis loops of Fig. 6.)

(3) In general base-course slip increases with the second and third cycles of any ductility level. The exception is A6 at DF = 4, where the base-slip contribution to total deflection decreased on the third cycle.

(4) The beneficial influence of vertical load in limiting slip is apparent when the behaviour of walls A3 and A6 is compared. Despite higher load levels and higher displacements at all ductility factors, slip is consistently less for A6, and the curves stiffen at an earlier displacement, presumably due to early closing of the base crack by the additional vertical load.

Cracking Behaviour.

All walls formed full diagonal shear cracks in each direction during the initial 'elastic' load cycles. However, the horizontal shear steel was in all cases sufficient to control the shear cracks elastically at all load levels. After unloading at the end of testing shear cracks were noted to have effectively closed up. Figs. 8a and 8b show typical photos of crack patterns after cycling at DF = 4.

Although the confining plates did not appear to significantly reduce stiffness degradation, as noted above, the amount of physical damage to the toe and heel areas was substantially reduced. Fig. 8c and 8d show the condition of wall ends of A1 and A3 (without and with confining plates respectively) after cycling at DF = 4. At this stage the unconfined wall (Fig. 8c) had suffered a complete separation of the toe from the body of the wall, but the confined wall (Fig. 8d) showed only comparatively minor cracking. This behaviour was typical of the other pairs of walls.

It was felt that all walls confined with mortar bed confining plates could have been adequately repaired after cycling to DF = 4 by raking out the base mortar joint and pumping in epoxy mortar. The unconfined walls would have required more substantial repair treatment.

5. DISCUSSION OF RESULTS

Flexural Capacity.

All walls exceeded their theoretical ultimate load capacities (P_u) based on measured steel yield stress, as a result of strain hardening of the flexural steel. Note that the design ultimate load for these walls based on an under-capacity factor $\phi = 0.65$ and nominal (414 MPa) rather than actual steel properties would have been about $0.6P_u$ for walls A2 and A4, and $0.5P_u$ for walls A1, A3, A5 and A6. Based on a yield stress of 380 MPa, the design loads would be correspondingly lower. Table 3 summarizes ultimate load capacities, where

P_u = Theoretical ultimate load

P_D = Design ultimate load $\phi = 0.65$, fy = 414 MPa

P_{EXP} = Max. experimental ultimate load

v_u = Shear stress at P_{EXP}

v_D = Max. code allowable shear stress

The average value of the ratio : maximum experimental load/theoretical capacity is

$$\left(\frac{P_{EXP}}{P_u}\right) \text{ ave} = 1.20$$

When compared with the design load P_D, the average ratio is

$$\left(\frac{P_{EXP}}{P_D}\right) \text{ ave} = 2.12$$

It thus appears that the design under-capacity factor of $\phi = 0.65$ may be excessively severe. It is significant that walls A2 and A4 (moderate rather than heavy steel percentage) exceeded P_D at all peaks, including three cycles to DF = 6 in both directions.

Shear Capacity.

No wall suffered a diagonal shear failure, despite maximum shear stresses many times higher than the maximum code level of 0.62 MPa. Shear design by carrying all shear force on horizontal steel was satisfactory in all cases, and it was apparent from examination of the walls after completion of testing that the shear steel did not yield in any wall. Adequate anchorage of shear steel was provided by hooking the ends of the steel around the extreme vertical bars.

Maximum experimental shear stresses based on the wall gross cross-sectional area are compared with the design value in Table 3. The maximum shear stress obtained was 2.62 MPa, or 4.22 x the maximum ultimate shear allowed on masonry walls. It is clear that the current shear limitations are quite unreasonably low.

Influence of Base-Course Slip.

At ductility factors of 4 and above, roughly half of the total wall displacement results from base-course slip. It would seem that if this could be eliminated, or substantially reduced, degradation at the higher ductility factors would be less severe. There are at least three feasible ways of reducing the base slip, each illustrated in Fig. 9.

The first, Fig. 9(a), suggested by Holmes, Wood, Poole and Johnstone, Consulting Engineers, Christchurch, involves building the wall on a foundation beam, then pouring the floor slab on top of the foundation beam round the wall, thus encasing the bottom course in the floor slab, inhibiting sliding. A disadvantage of this method is that in some cases (perimeter or free-standing walls) it may be difficult to provide sufficient restraint. Also, substantial additional reinforcing steel would be required in the slab close to the wall base to cope with the high tensions across the potential cracks (see plan, Fig. 9(a)).

The second method, Fig. 9(b), would involve angle-section or channel-section starters protruding from the foundation beam up to two or three courses into the blockwork. The greatly increased stiffness of the angle or channel would be more efficient than the vertical bars in dowel action, and since they would not be subjected to tensile yield, would not be subject to reduction in stiffness due to the Bauschinger effect. A 45 x 45 x 7.9mm angle section, which could easily be accommodated in a 190mm block wall has 2.3 x the area of a 19mm dia bar, but is 27 x stiffer than a 19mm bar, in the configuration adopted in Fig. 9(b) which also produces minimum congestion. Dowel angles or channels should be concentrated in the central portion of the wall rather than the ends to avoid pushing out the end-blocks.

The third method, Fig. 25(c) suggested by Professor Paulay of the University of Canterbury would involve diagonal reinforcement of the base-course joint. A strip of (e.g.) HRC mesh bent to form a continuous zig-zag would be cast half into the foundation beam, and half into the grout core. The transverse link bars would tend to hold the enclosed concrete intact. Since it is common practice to use inverted bond beam blocks in the lower course to facilitate clean-out operations, no special problems in placing should arise. However, the

amount of shear that can be transferred by reasonable sized bars (say up to 6mm dia.) in this method is comparatively small.

It is the writers opinion that the second method is likely to be the most successful and easiest to accomplish in practice. Both other methods protect only the base-course sliding, and it was noted that sliding occurred at the second course during the later stages of test for each wall. If base slip is eliminated the rotational ductilities sustained by the walls would be higher, and the tendency would be for slip to occur at the next course at an earlier stage of testing. Improvement of behaviour would be expected, but the extent of improvement is difficult to predict.

Finally, it is emphasized that degradation due to base-course slip tends to occur at the same ductility level, not at the same load, for each wall. At DF = 2 behaviour of all walls was satisfactory. At DF = 4, all walls exhibited sliding degradation, though the more lightly reinforced walls (A2 and A4) did not degrade as rapidly, nor to the same extent. Sliding will not occur until flexural cracks have reached substantial widths due to large inelastic steel strains. Note that the dowel resistance to sliding will be proportional to the number and diameter of vertical bars, and thus will generally be roughly proportional to the ultimate flexural capacity of the wall. This can be seen from Fig. 6, where the sliding resistance at zero load for A3 is about twice that for A4. The presence of vertical load in A6 further increases the sliding resistance.

In conclusion, the concept of a limiting shear friction does not appear to be valid.

Elastic Stiffness

It is the writer's belief that current values adopted for the elastic stiffness of masonry walls are too high, resulting in fundamental frequencies, and therefore code base shear coefficients that may also be too high. Current practice is to base period calculations on a Modulas of Elasticity of about 10GPa, and use of the uncracked-section Moment of Inertia. Theoretical yield displacements for walls A1, A2 and A5, including both flexural and shear terms based on the above assumption are compared with measured displacements in Table 4.

It appears from these results that taking a cracked stiffness equal to half of the uncracked stiffness for both flexural and shear modes would result in conservative values for the elastic cracked stiffness, resulting in building periods approximately 40% higher than is currently adopted. The most simple method of incorporating this change would be to assume an effective Modulus of Elasticity of 5.0 GPa, using uncracked section properties.

It should also be noted that most masonry buildings will be subject to considerable foundation flexibility, further increasing yield displacements, and reducing building periods.

Comparison of Available and Required Ductility

It is of interest to compare required ductility for an actual example with the values obtained from the tests reported in Section 4. Consider the 5 storey masonry building sketched in Fig. 10. The seismic resistance in the NS direction is provided by shear walls at each end. It is assumed that the building is located in Zone A on rigid subsoil. Calculations indicate a natural period of about 0.43 sec. based on the recommendations of the section above. As in section 1.1 the seismic coefficient will be Cd = .288. The building is designed for a live load of L = 5.0 kPa, resulting in an effective mass (DL + Seismic LL) of 400 tonnes/floor.

The roof is assumed to have half the weight of a floor, so the distribution of mass is as given in Fig. 10 (b). Thus the total mass is

$$M_T = 4.5 \times 400 = 1800 \text{ tonnes and}$$

$$\text{Base shear } V = .288 \times 1800 \times 9.8$$

$$= 5.08 \text{ MN}$$

$$= \underline{2.54 \text{ MN/wall}}$$

Assuming block width = 190mm, the base shear stress will be

$$v = \frac{2.54}{15 \times .19}$$

$$= \underline{0.89 \text{ MPa}}$$

As mentioned in Section 1, the maximum allowable shear stress at design base shear coefficient is about 0.30 MPa, because of undercapacity factors and likely over-strength. Consequently shear in this example is roughly three times the maximum permitted. Nevertheless we will proceed on the assumption this is acceptable.

Thompson[10] in a recent Ph.D. thesis investigated the influence of different hysteresis loops, including elastic, elasto-plastic, degrading stiffness and degrading stiffness-slip, combined with natural periods from 0.3 sec to 2.1 sec, on the maximum displacement ductility factors under El Centro 1940 NS Earthquake. As mentioned above, the degrading stiffness model appears best to fit the behaviour observed in these tests, for ductility factors less than or equal to 4. Thompson's values were based on lower values of C_d than used in this example, so in applying his results, the required ductilities may be factored down by the ratio of Thompson's base shear coefficient/0.288. This is effectively the 'equal-displacement' principal inverted, which is a conservative assumption since the principle is non-conservative for required ductilities for low period structures. Values are listed in Table 5 for 'dependable' and 'ideal' strengths for 0.3 sec. and 0.6 sec. period assuming damping of 5%, and are interpolated linearly for 0.43 sec. On the basis of these results the required ductility is likely to be less than 2.7 due to the conservative nature of the assumptions made. Even based on the very conservative 'dependable' strength, the required ductility should only be about 4. The tests reported above show that the level of ductility is satisfactory for walls subjected to maximum shear stresses of about 1.2 MPa. For walls with maximum shear stresses exceeding 2.0 MPa

the demands might be too high.

6. CONCLUSIONS AND DESIGN RECOMMENDATIONS

Diagonal Shear

The main purpose of these tests was to demonstrate that the limits imposed on maximum shear stress by the Masonry code are unrealistically low. This has clearly been achieved, as all walls exceeded the maximum permitted value by substantial margins, with two walls exceeding 4 times the code level. No wall showed any signs of distress as a result of high diagonal shear stresses. It is thus concluded that provided all shear is carried by adequately anchored horizontal steel, higher shear stresses should be allowed. It is recommended that

(1) Maximum shear stresses of 1.25 MPa, based on the gross cross-section of the wall should be allowed for concrete masonry walls expected to sustain displacement ductility factors up to 4. This would include walls designed to current NZS 4203 levels of base shear.

(2) Higher shear stresses, up to 2.5 MPa should be allowed provided displacement ductility factors will not exceed 2. This would require design to higher base shear coefficients than specified by NZS 4203. These requirements are intended to limit base-course slip, and there seems little justification to tying the shear strength to the masonry crushing strength.

Undercapacity Factor for Flexure

The current undercapacity factor[2] for walls subjected to axial compression and bending is $\phi = 0.65$. In all walls tested in this series the theoretical ultimate moment capacity based on measured material properties were substantially exceeded, the average excess being 20%, despite the high shear stresses. It is felt that a higher value for ϕ is warranted. This would conform with current thinking for the undercapacity factor for column members in frames, where it is suggested that the ϕ factor should be increased from 0.7 to 0.9.

Consequently it is recommended that the undercapacity factor for masonry walls subjected to flexure and axial load should be increased from 0.65 to 0.85.

Degradation

All walls behaved in satisfactory fashion at displacement ductility factors of 2, and the two less heavily reinforced walls were satisfactory at DF = 4. Degradation occurred at higher ductilities due to slipping of the wall along the top of the foundation beam. It is felt that behaviour could be further improved by inhibiting base-course slip. Methods for achieving this should be tested. Some possibilities are suggested.

Results from inelastic analyses indicate that ductilities required for walls designed to NZS 4203 should be less than 4.

Elastic Stiffness

The test results indicate that current design practice overestimates the cracked stiffness of walls by a factor of more than 2. It is recommended that yield displacements and building periods should be based on the uncracked section, using an effective Modulus of Elasticity of 5 GPa.

Confining Plates

Mortar-bed confining plates did not significantly reduce stiffness degradation in the walls of this test series. However, damage control and condition for wall repair after a major earthquake were improved by the inclusion of the plates. It is possible that the comparatively high mortar strength in the walls reduce the mismatch in material properties between block and mortar, thus reducing the tendency for compression splitting of the blockwork. Further tests are advisable to check this point.

Vertical Load

Walls subjected to moderate vertical loading (0.69 MPa) behaved better than walls without vertical load. Base-course slip was reduced, and degradation at DF = 4 was less severe.

7. ACKNOWLEDGEMENTS

The assistance, financially and during manufacture and testing of the walls, of Winstones S.I. Ltd., is gratefully acknowledged. The test programme was conceived and designed in conjunction with the Christchurch based consulting firm, Holmes, Wood, Poole and Johnstone.

8. REFERENCES

1. Standard Ass. of N.Z. "NZSS 1900 Design and Construction, Chapter 9.4 Masonry", 1962.
2. Proposed draft, Standards Ass. of N.Z. "Code of Practice for Masonry Buildings, Part B" DZ4210.
3. Standards Ass. of N.Z. "Code of Practice for General Structural Design and Design Loadings for Building" NZS4203:1976.
4. Scrivener, J.C., "Static Racking Tests on Concrete Masonry Walls", Proc. Int. Conf. on Masonry Structural Systems, Texas, Nov. 1967.
5. Schneider, R. R., "Lateral Load Tests on Reinforced Grouted Masonry Shear Walls", Univ. of Sthn. Calif. Eng. Centre, Rept. 70-101, Sept. 1959.
6. Priestley, M.J.N. and Bridgeman, D.O., "Seismic Resistance of Brick Masonry Walls", Bull. N.Z. Nat. Soc. for Earthquake Eng., Vol. 7, No. 4, Dec. 1974, pp 167-187.
7. Paulay, T., "Design Aspects of Shear Walls for Seismic Areas", Univ. of Canterbury, Dep. of Civil Eng., Research Report 74-11, Oct. 1974, 29pp.
8. Priestley, M.J.N., "Cyclic Testing of Heavily Reinforced Concrete Masonry Shear Walls", Univ. of Canterbury, Dept. of Civil Eng., Research Report 76-12, Oct. 1976, 75pp.
9. Clough, R. W., "Effect of Stiffness Degradation on Earthquake Ductility Requirements", Univ. of Calif. Struct. Eng. Lab. Report No. 66-16, Oct. 1966, 66 pp.
10. Thompson, K. J., "Ductility of Concrete Frames Under Seismic Loading", Ph.D.

Thesis, Univ. of Canterbury, Civil Eng. Dept., Research Report No. 75-14, Oct. 1975, 341 pp and Appendices.

TABLE 1

UNIT REINFORCING DETAILS

Unit	Vertical Reinforcing	Shear Reinforcing	Confining Plates	Vertical Load
A1	8/19.05mm	8/19.05mm	No	-
A2	6/15.9mm	8/15.9mm	No	-
A3	8/19.05mm	8/19.05mm	Yes	-
A4	6/15.9mm	8/15.9mm	Yes	-
A5	8/19.05mm	8/19.05mm	No	240 kN
A6	8/19.05mm	8/19.05mm	Yes	240 kN

Note all reinforcing steel grade 380.

TABLE 2

MATERIAL STRENGTHS

Wall	REINFORCING TENSILE ST. (MPa)				BLOCKWORK CRUSHING STRENGTH (MPa)			
	FLEXURAL STEEL		SHEAR STEEL					
	YIELD	ULT	YIELD	ULT	BLOCKS	MORTAR	GROUT	PRISMS
A1	528	871	505	841	30.7	37.9	24.8	19.3
A2	432	711	421	664	30.7	42.9	24.8	18.3
A3	474	782	513	855	30.7	32.4	24.8	20.4
A4	454	722	427	679	30.7	32.5	24.8	21.2
A5	488	802	489	814	30.7	33.5	24.8	18.3
A6	472	780	488	805	30.7	38.7	24.8	24.5

TABLE 3

ULTIMATE LOADS OF WALLS

WALL	MAX. LOADS (kN)					MAX. SHEAR STRESS (MPa)		
	P_u	P_D	P_{EXP}	$\frac{P_{EXP}}{P_T}$	$\frac{P_{EXP}}{P_D}$	v_u	v_D	$\frac{v_u}{v_D}$
A1	695	367	771	1.11	2.10	2.21	0.62	3.56
A2	330	204	409	1.24	2.00	1.17	0.62	1.89
A3[1]	652	367	733	1.12	2.00	2.10	0.62	3.38
A4[1]	330	204	460	1.39	2.25	1.32	0.62	2.13
A5*	818	418	915	1.12	2.19	2.62	0.62	4.22
A6[1]*	734	418	911	1.24	2.19	2.61	0.62	4.21

1. Confining plates

* Vertical Load = 240 kN

TABLE 4

THEORETICAL AND EXPERIMENTAL YIELD DISPLACEMENT

WALL	P_u (kN)	Δ_{Theor} (mm)	Δ_{exp} (mm)	$\frac{\Delta_{exp}}{\Delta_{Theor}}$
A1	695	2.19	5.0	2.28
A2	330	1.04	3.33	3.20
A5	818	2.58	6.0	2.33

TABLE 5

BUILDING EXAMPLE. REQUIRED DISPLACEMENT DUCTILITIES

(EL CENTRO 1940 NS)

PERIOD (sec)	REQUIRED DUCTILITIES	
	'Dependable' strength ϕ = 0.65	'Ideal' strength ϕ = 1.0
0.3	5.2	3.4
0.6	2.7	1.7
0.43	4.1	2.7

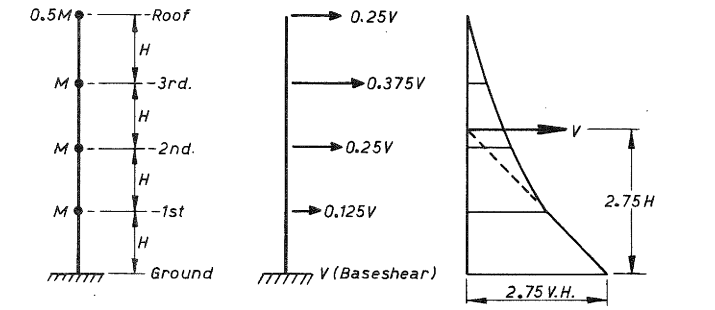

FIGURE 1: :POSITION OF EQUIVALENT LOAD FOR CORRECT MOMENTS AND SHEARS IN 4-STOREY BUILDING

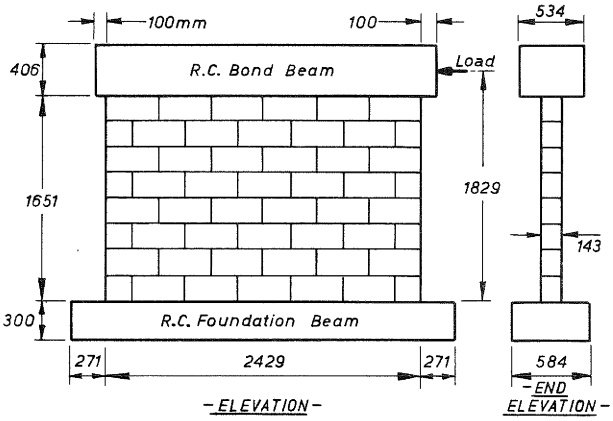

FIGURE 2: TEST WALL DIMENSIONS

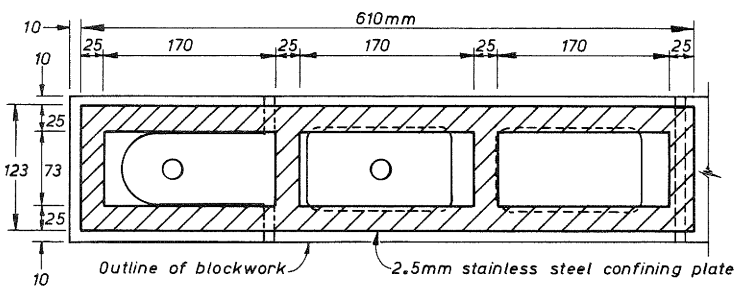

FIGURE 3: MORTAR BED CONFINING PLATES FOR A3, A4 AND A6

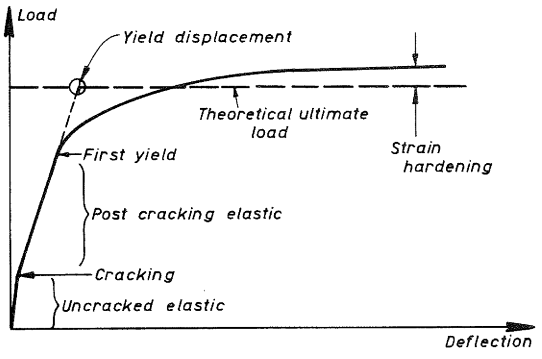

FIGURE 5: DEFINITION OF YIELD DISPLACEMENT

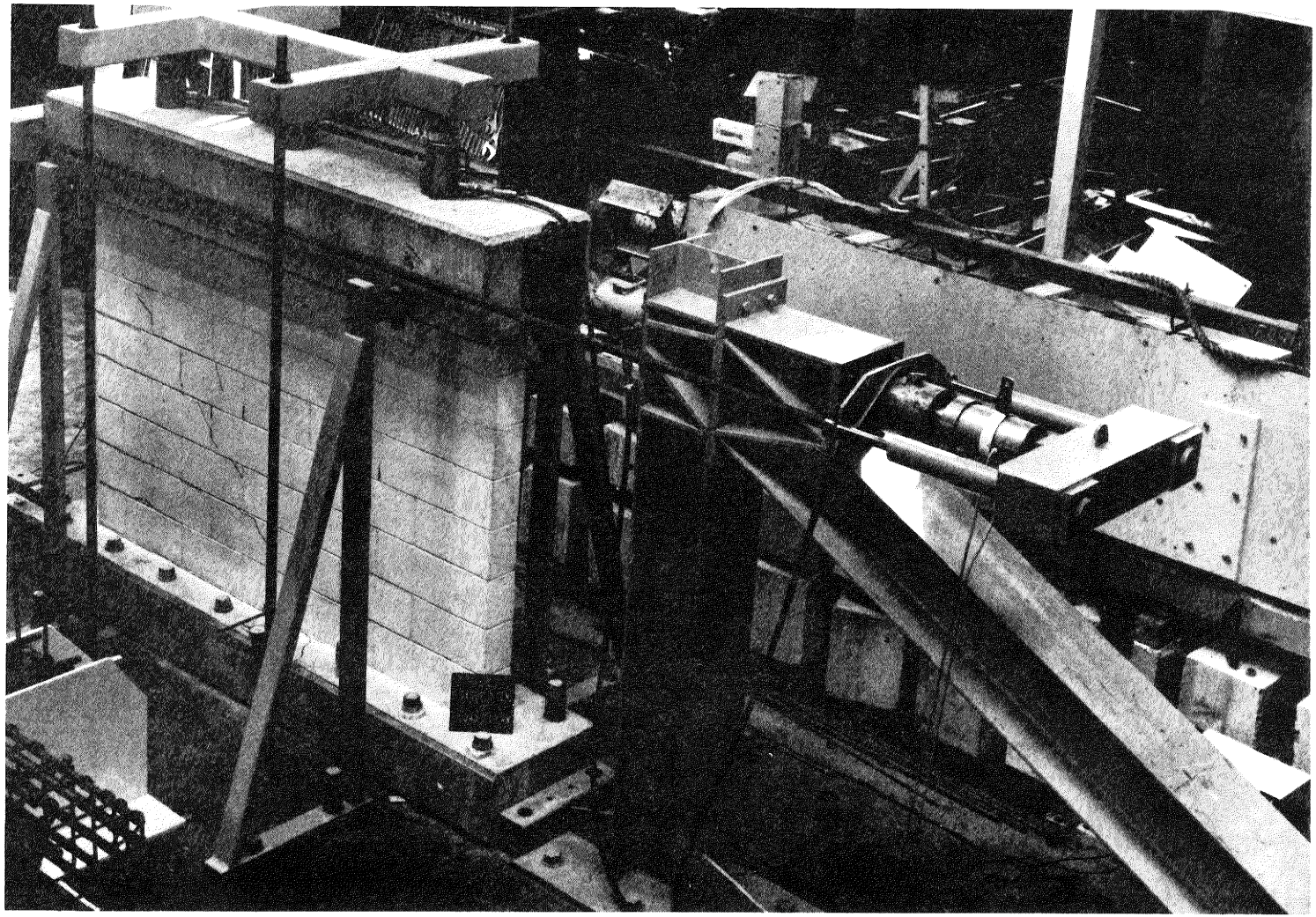

FIGURE 4: WALL WITH VERTICAL LOAD UNDER 'TENSION' LOADING

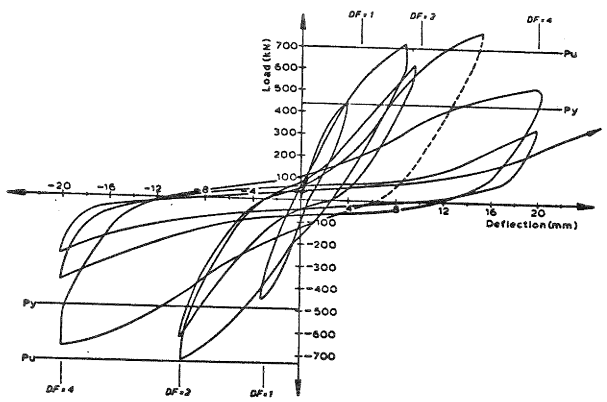

(a) Wall A1

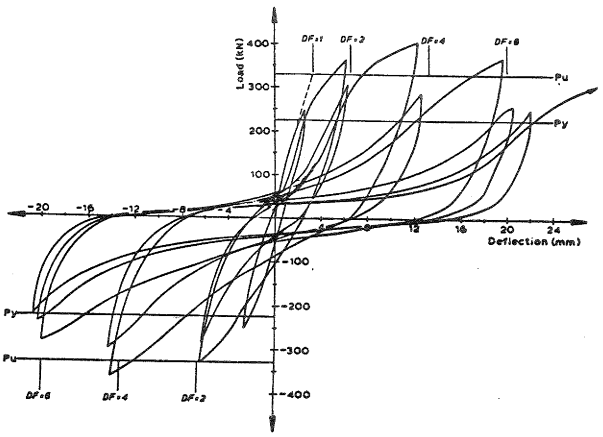

(b) Wall A2

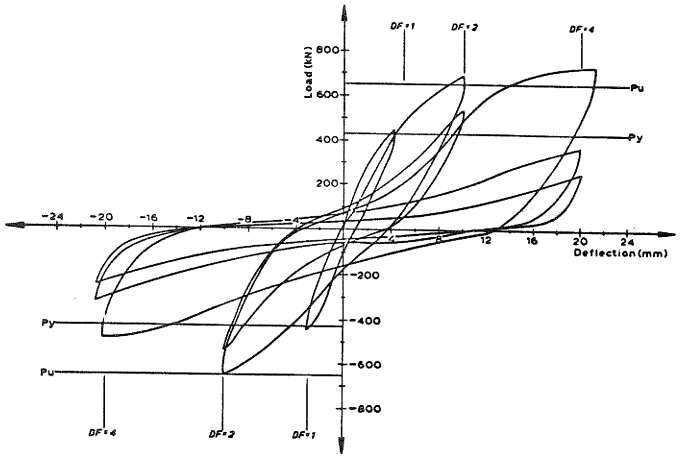

(c) Wall A3

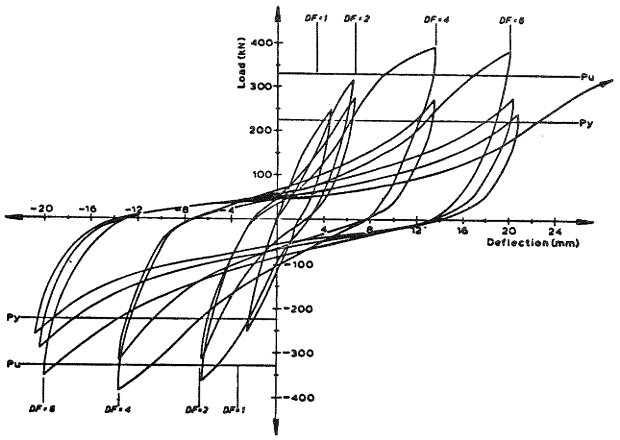

(d) Wall A4

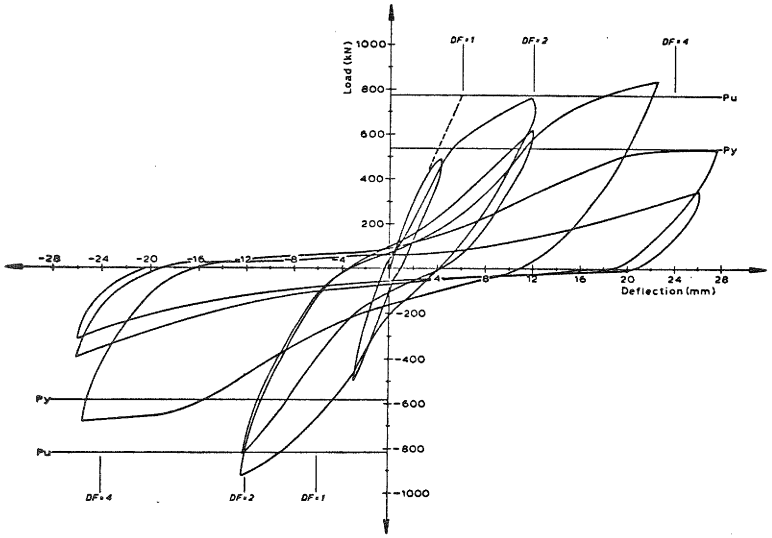

(e) Wall A5

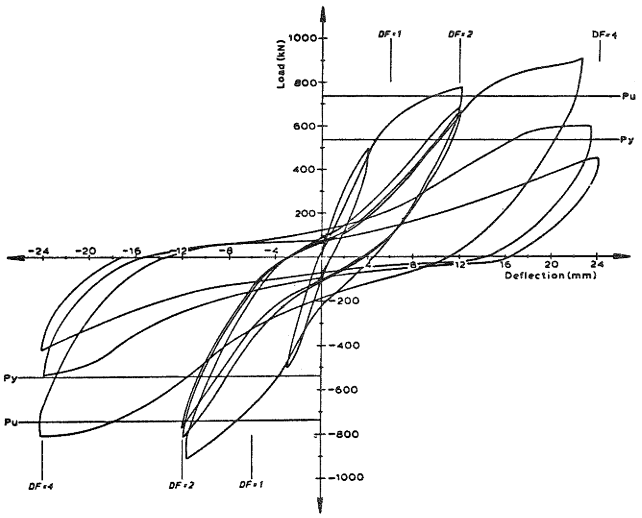

(f) Wall A6

FIGURE 6: LOAD-DEFLECTION HYSTERESIS LOOPS

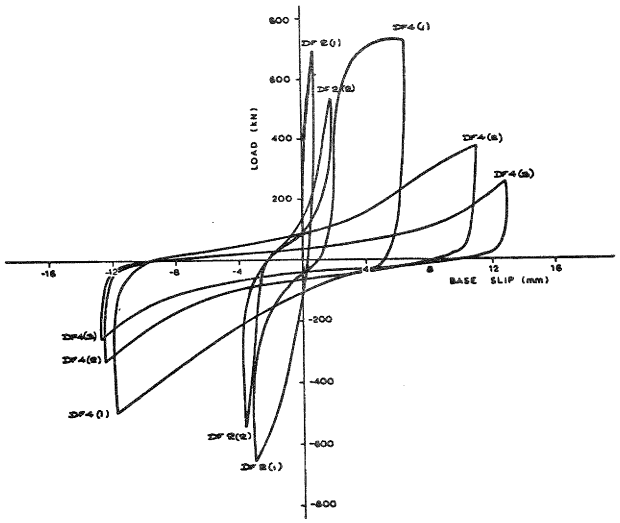

(a) Wall A3

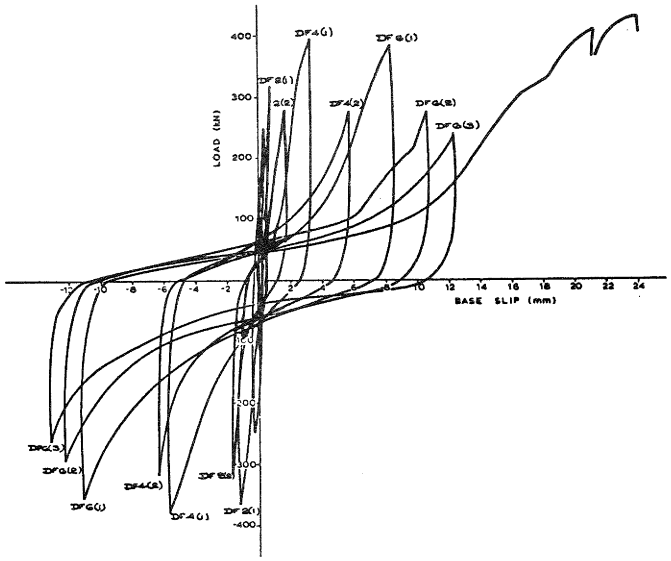

(b) Wall A4

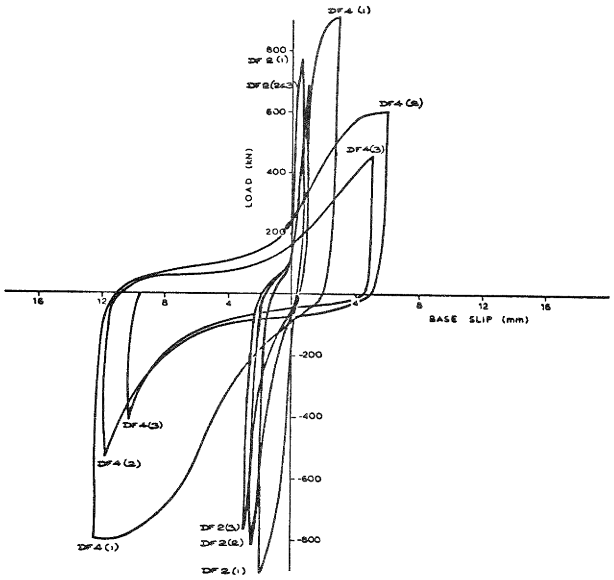

(c) Wall A6

FIGURE 7: LOAD/BASE-SLIP HYSTERESIS LOOPS

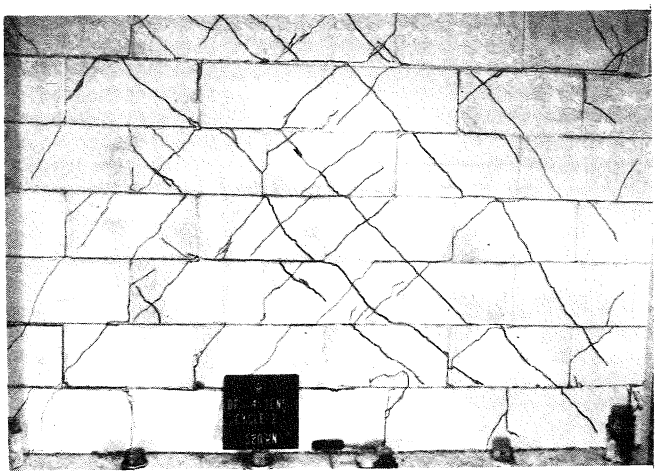

(a) A1 Condition at DF = 4

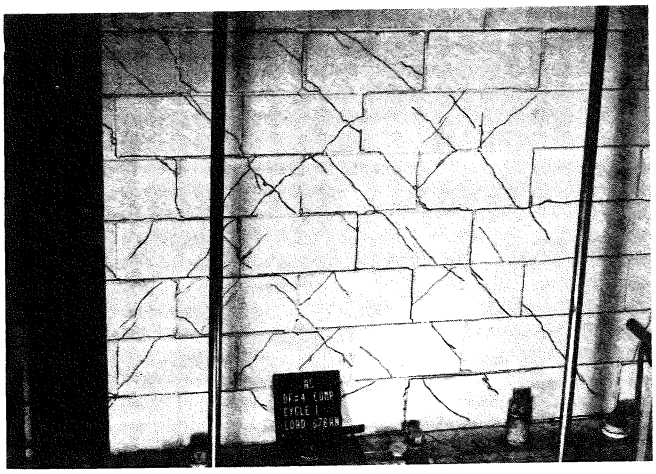

(b) A5 Condition at DF = 4

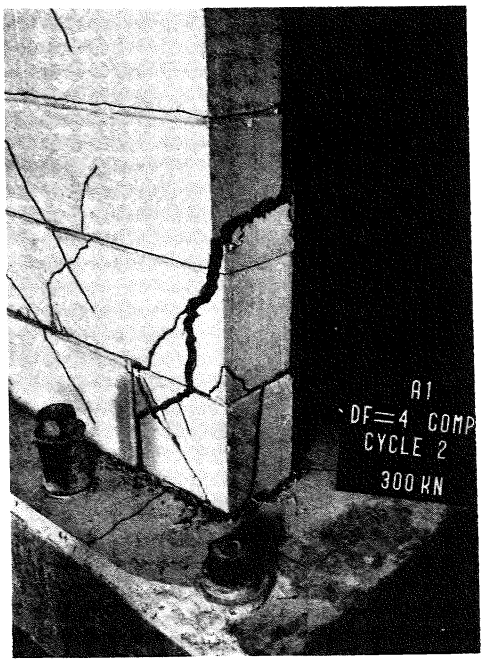

(c) A1 End Vertical Crack, DF = 4

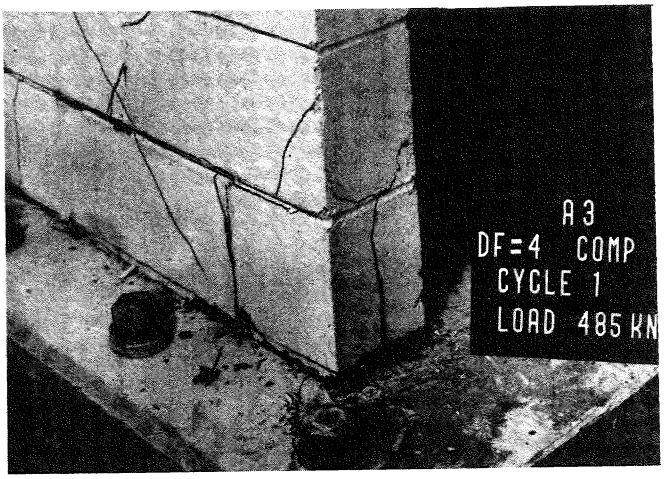

(d) A3 End of Wall at DF = 4

FIGURE 8: PHOTOS OF CRACK PATTERNS

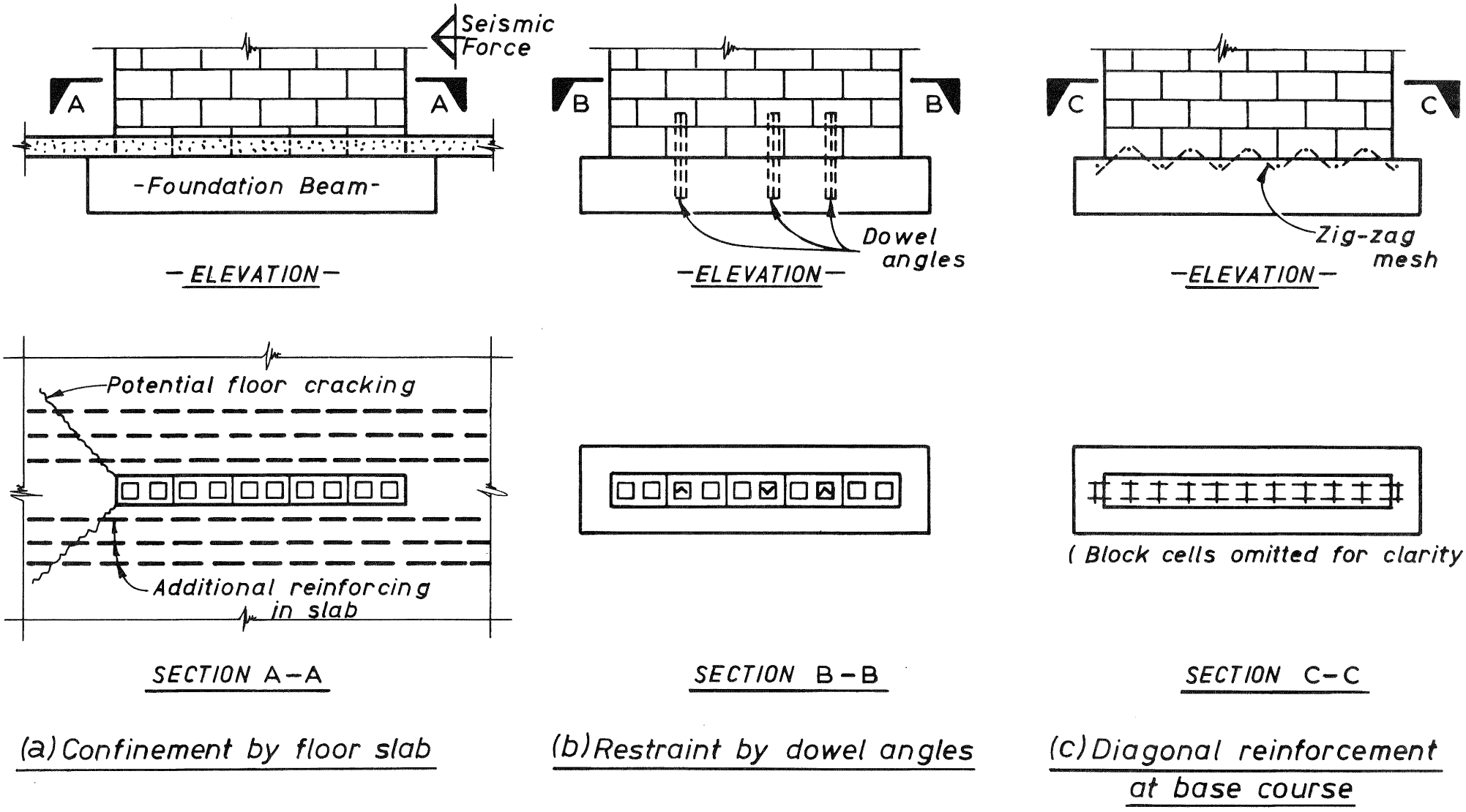

FIGURE 9: METHODS FOR REDUCING BASE-SLIP

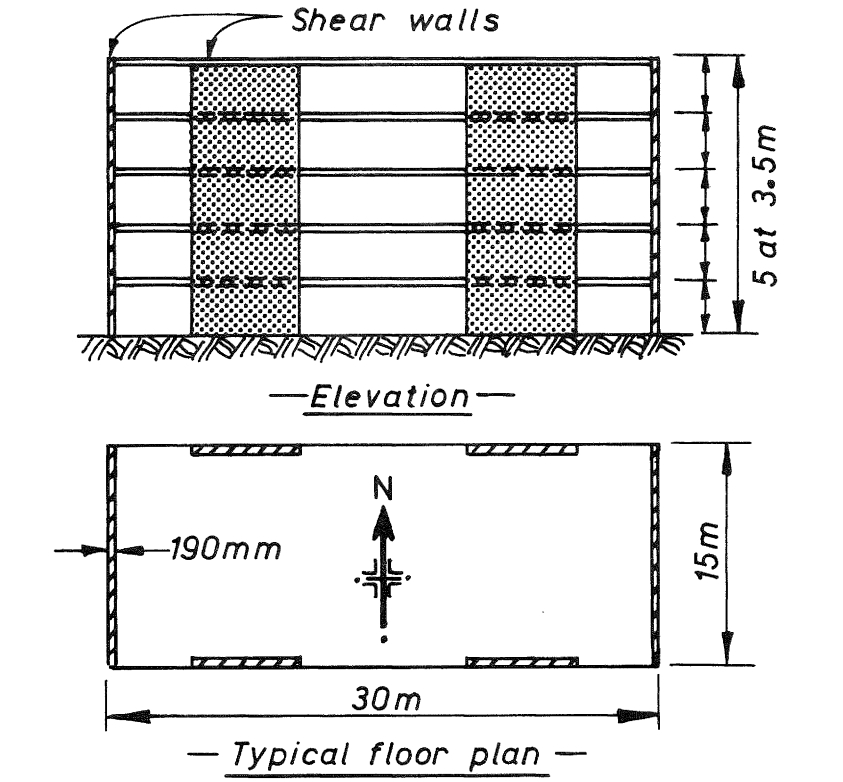

FIGURE 10: MASONRY BUILDING EXAMPLE